

ORIGINAL ARTICLE

# Transcriptional repression of IFN $\beta$ 1 by ATF2 confers melanoma resistance to therapy

E Lau<sup>1</sup>, J Sedy<sup>1</sup>, C Sander<sup>2</sup>, MA Shaw<sup>3</sup>, Y Feng<sup>1</sup>, M Scortegagna<sup>1</sup>, G Claps<sup>1</sup>, S Robinson<sup>4</sup>, P Cheng<sup>5</sup>, R Srivas<sup>6</sup>, S Soonthornvacharin<sup>1</sup>, T Ideker<sup>7</sup>, M Bosenberg<sup>8</sup>, R Gonzalez<sup>4</sup>, W Robinson<sup>4</sup>, SK Chanda<sup>1</sup>, C Ware<sup>1</sup>, R Dummer<sup>5</sup>, D Hoon<sup>3</sup>, JM Kirkwood<sup>2</sup> and ZA Ronai<sup>1</sup>

The resistance of melanoma to current treatment modalities represents a major obstacle for durable therapeutic response, and thus the elucidation of mechanisms of resistance is urgently needed. The crucial functions of activating transcription factor-2 (ATF2) in the development and therapeutic resistance of melanoma have been previously reported, although the precise underlying mechanisms remain unclear. Here, we report a protein kinase C- $\epsilon$  (PKC $\epsilon$ )- and ATF2-mediated mechanism that facilitates resistance by transcriptionally repressing the expression of interferon- $\beta$ 1 (IFN $\beta$ 1) and downstream type-I IFN signaling that is otherwise induced upon exposure to chemotherapy. Treatment of early-stage melanomas expressing low levels of PKC $\epsilon$  with chemotherapies relieves ATF2-mediated transcriptional repression of IFN $\beta$ 1, resulting in impaired S-phase progression, a senescence-like phenotype and increased cell death. This response is lost in late-stage metastatic melanomas expressing high levels of PKC $\epsilon$ . Notably, nuclear ATF2 and low expression of IFN $\beta$ 1 in melanoma tumor samples correlates with poor patient responsiveness to biochemotherapy or neoadjuvant IFN- $\alpha$ 2a. Conversely, cytosolic ATF2 and induction of IFN $\beta$ 1 coincides with therapeutic responsiveness. Collectively, we identify an IFN $\beta$ 1-dependent, cell-autonomous mechanism that contributes to the therapeutic resistance of melanoma via the PKC $\epsilon$ -ATF2 regulatory axis.

*Oncogene* (2015) 34, 5739–5748; doi:10.1038/onc.2015.22; published online 2 March 2015

## INTRODUCTION

Human melanoma, characterized by aggressive metastatic behavior and the ability to rapidly develop therapeutic resistance, represents one of the most lethal forms of skin cancer. Despite the advent of effective targeted monotherapies, such as the mutant B-RAF kinase inhibitors vemurafenib (PLX4720) and dabrafenib, most melanomas eventually develop therapeutic resistance that drives relapse and progression.<sup>1</sup> A number of studies have identified genetic and epigenetic mechanisms through which melanomas can acquire resistance to mutant B-RAF inhibitors, including mutation of RAS, MAP2K1 and ERK, and upregulation of PDGFR and MAP3K8<sup>2–4</sup>—all of which contribute to reactivation of the mitogen-activated protein kinase/extracellular-signal-regulated kinase signaling pathway. Other therapeutic modalities for melanoma include agents that inhibit immune response checkpoints, such as CTLA-4 (cytotoxic T-lymphocyte-associated protein 4)<sup>5–7</sup> and PD1 (programmed cell death protein 1),<sup>8,9</sup> and immunomodulatory cytokines such as interleukin-2 (IL-2) and interferon (IFN)- $\alpha$ 2a<sup>10</sup> have exhibited variable efficacy. In addition, chemo- and biochemotherapeutic regimens (for example, chemotherapeutic agents cisplatin, vinblastine or dacarbazine, alone or in combination with IFN- $\alpha$ 2a or IL-2), have been limited in efficacy and are considered as palliative modalities for late-stage metastatic melanoma patients.<sup>11–13</sup> In general, the overall therapeutic success for melanomas has been limited by our insufficient understanding of mechanisms—beyond the mitogen-activated protein kinase signaling pathway—that facilitate resistance and by

our inability to identify patients who might be most responsive to specific therapies.

Activating transcription factor-2 (ATF2), a member of the activator protein-1 (AP1) helix-loop-helix transcription factor family, elicits both oncogenic and tumor suppressor functions, depending on its subcellular localization. We previously reported that in melanoma cells subjected to genotoxic stress (a common outcome of most anticancer therapies), ATF2 localizes to the cytoplasm where it acts as a tumor suppressor by perturbing the VDAC1/HK1 (voltage-dependent anion channel 1/hexokinase 1) complex at the mitochondrial outer membrane and promoting apoptosis.<sup>14</sup> In contrast, phosphorylation of ATF2 on threonine 52 (T52) by protein kinase C- $\epsilon$  (PKC $\epsilon$ ) promotes the nuclear localization and transcriptional activity of ATF2, rendering the cells resistant to chemotherapeutic stress. In successive stages of melanoma progression, levels of both PKC $\epsilon$  and nuclear ATF2 are increased and correlate with poorer clinical outcome,<sup>14</sup> suggesting that the PKC $\epsilon$ -ATF2 signaling axis contributes to tumorigenesis and chemoresistance. Notably, PKC $\epsilon$  was previously identified among the top 10 kinases that can confer resistance to BRAF inhibition in melanoma<sup>2</sup> and, importantly, a recent study identified ATF2 as a crucial mediator of resistance to Sorafenib in liver cancer, demonstrating that loss of ATF2 is sufficient to revert resistance.<sup>15</sup> Consistent with this notion, synthetic peptides or small-molecule inhibitors that attenuate the phosphorylation of ATF2 by PKC $\epsilon$ , promote its cytoplasmic localization, and thus inhibit its transcriptional activity, can sensitize melanoma cells to

<sup>1</sup>Cancer Center, Sanford-Burnham Medical Research Institute, La Jolla, CA, USA; <sup>2</sup>University of Pittsburgh Cancer Center, Pittsburgh, PA, USA; <sup>3</sup>John Wayne Cancer Institute, Santa Monica, CA, USA; <sup>4</sup>Division of Medical Oncology, University of Colorado Anschutz Medical Campus, Aurora, CO, USA; <sup>5</sup>Department of Dermatology, University of Zurich, Zurich, Switzerland; <sup>6</sup>Department of Genetics, Stanford University School of Medicine, Palo Alto, CA, USA; <sup>7</sup>Department of Medicine, University of California, San Diego, San Diego, CA, USA and <sup>8</sup>Yale School of Medicine, New Haven, CT, USA. Correspondence: Dr E Lau or Dr ZA Ronai, Cancer Center, Sanford-Burnham Medical Research Institute, 10901 North Torrey Pines Road, La Jolla 92037, CA, USA.

E-mail: elau@sbmri.org or ronai@sbmri.org

Received 7 October 2014; revised 2 January 2015; accepted 6 January 2015; published online 2 March 2015

death.<sup>16,17</sup> However, the precise transcriptional program coordinated by PKC $\epsilon$  and ATF2 to drive chemoresistance is not yet known. Here, we report that the PKC $\epsilon$ -ATF2 signaling axis facilitates resistance in melanoma by repressing the tumor-suppressive, therapeutic stress-induced expression of IFN $\beta$ 1.

**RESULTS**

**PKC $\epsilon$ -ATF2 signaling represses chemotherapy-induced IFN $\beta$ 1 expression**

We previously showed that phosphorylation of ATF2 by PKC $\epsilon$  on threonine 52 (pATF2) promotes its nuclear retention and transcriptional activation in melanoma cells, conferring resistance to chemotherapeutic stress.<sup>14</sup> Indeed, the expression of either the phosphomimic ATF2<sup>T52E</sup> or a constitutively active form of PKC $\epsilon$  (caPKC $\epsilon$ ) renders WM793 melanoma cells resistant to the chemotherapeutic (genotoxic) stress induced by etoposide (ETO)

or cisplatin (CIS), reducing cell death by ~50% (Figure 1a and Supplementary Figure 1a, lower;<sup>14</sup>). To determine the mechanism by which activation of the PKC $\epsilon$ -ATF2 signaling axis impacts chemotherapeutic resistance, we performed gene expression profiling of WM793 cells that were first depleted of endogenous ATF2 and then reconstituted with either ATF2<sup>T52E</sup> or the nonphosphorylatable mutant ATF2<sup>T52A</sup> that is predominantly cytoplasmic/mitochondrial and is transcriptionally inactive<sup>14</sup> (Supplementary Figure 1b). We identified the top 100 genes that were significantly upregulated or downregulated upon ETO treatment of ATF2<sup>T52E</sup>-expressing compared with ATF2<sup>T52A</sup>-expressing cells (Supplementary Table 1). Of these genes, IFN signaling was identified as the most significantly altered canonical signaling pathway (Supplementary Figure 1b, left), in which IFN $\beta$ 1 and the IFN-related genes *SP110*, *IRF9* and *IFI144L* were significantly downregulated in ETO-treated ATF2<sup>T52E</sup>-expressing cells (Supplementary Figure 1b, right)—suggesting that pATF2

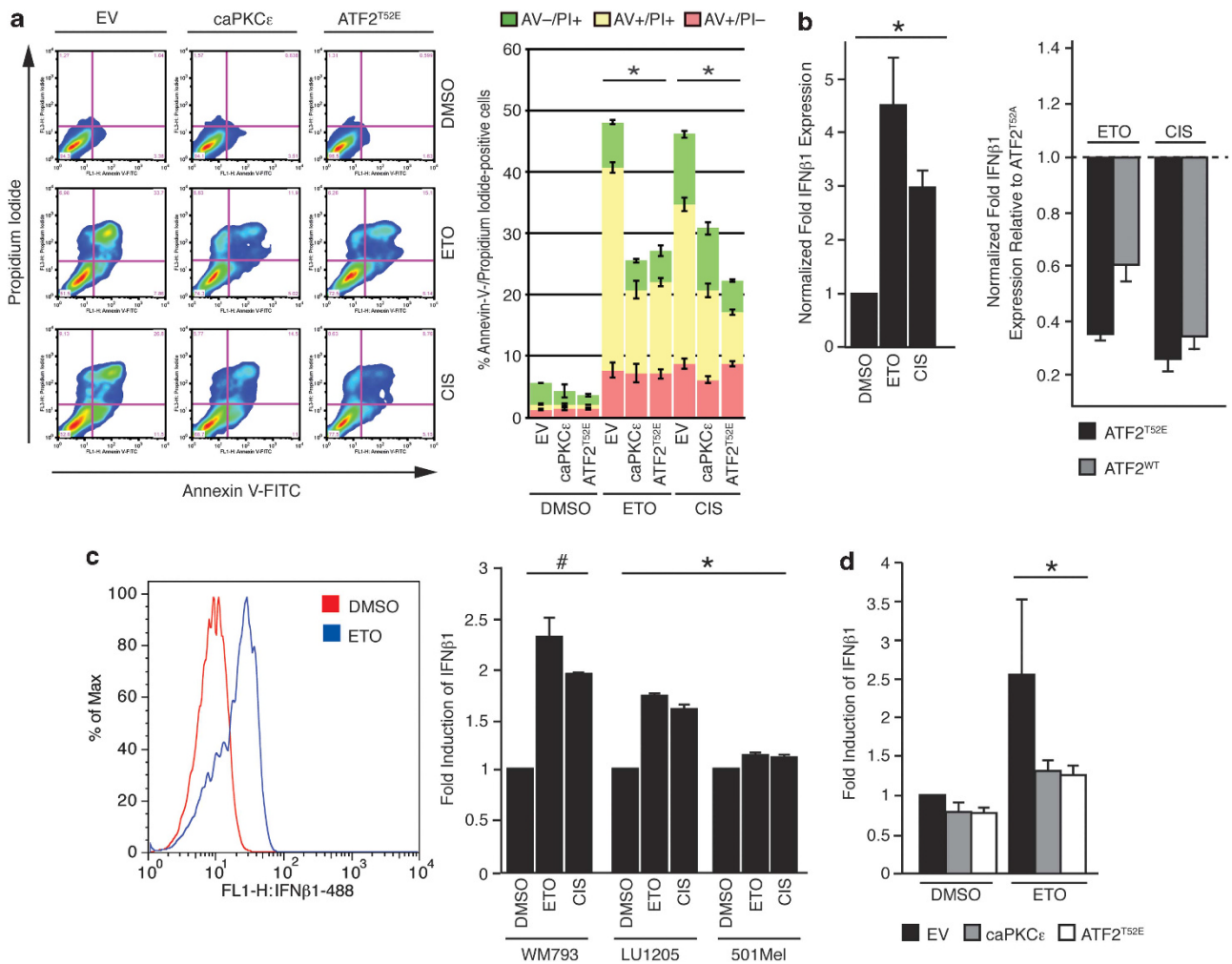


**Figure 1.** PKC $\epsilon$ -phosphorylated ATF2 confers chemotherapeutic stress resistance and reduces IFN $\beta$ 1 expression. (a, left) Representative Annexin-V (AV)/propidium iodide (PI) fluorescence-activated cell sorting (FACS) plots of WM793 melanoma cells transfected with empty vector (EV), ATF2<sup>T52E</sup> or constitutively active PKC $\epsilon$  (caPKC $\epsilon$ ) for 48 h and treated with dimethyl sulfoxide (DMSO), 10  $\mu$ M ETO or 10  $\mu$ M CIS for 24 h. (a, right) Quantitation of Annexin-V- and/or PI-positive cells. \**P* < 0.01. (b, left) Quantitative real-time reverse transcription-PCR (qRT-PCR) analysis of IFN $\beta$ 1 expression in WM793 cells treated with ETO or CIS normalized to levels in DMSO-treated cells. (b, right) qRT-PCR analysis of IFN $\beta$ 1 transcripts in ATF2-depleted WM793 cells reconstituted with ATF2<sup>WT</sup>, ATF2<sup>T52A</sup> or ATF2<sup>T52E</sup> for 48 h and then treated with ETO or CIS for 24 h. The IFN $\beta$ 1 transcript levels shown are relative to cells reconstituted with ATF2<sup>T52A</sup>. (c, left) Representative FACS histogram showing intracellular IFN $\beta$ 1 protein expression in DMSO-, ETO- and CIS-treated WM793 cells. (c, right) FACS quantification of induction of intracellular IFN $\beta$ 1 for WM793, LU1205 and 501Mel cells treated with DMSO or ETO. (d) Intracellular IFN $\beta$ 1 protein levels in WM793 cells expressing EV, caPKC $\epsilon$  or ATF2<sup>T52E</sup> and treated with DMSO or ETO. \**P* < 0.05; #*P* = 0.0032. The results shown represent the mean values  $\pm$  s.d. of experiments performed in biological triplicate.

represses IFN pathway components. Quantitative real-time reverse transcription–PCR analysis of IFN $\beta$ 1 transcripts confirmed that ETO and CIS treatments increased IFN $\beta$ 1 mRNA levels by ~4- to 5-fold and ~3-fold, respectively, in WM793 cells (Figure 1b, left). This induction of IFN $\beta$ 1 by ETO or by CIS was reduced by ~60–70% or ~40–60% by the expression of ATF2<sup>T52E</sup> or wild-type ATF2, respectively (Figure 1b, right). Consistent with these observations, ETO treatment increased the expression of both IFN $\beta$ 1 and SP110 by ~4- to 5-fold in melanoma cells with low levels of PKC $\epsilon$ /pATF2 (WM793) and by ~2-fold in cells with intermediate levels (LU1205), but had no effect in cells with high levels of PKC $\epsilon$ /pATF2 (501Mel; Supplementary Figures 1a and c–e). This relationship between PKC $\epsilon$ /pATF2 levels and IFN-related gene expression was also observed for the downstream IFN $\beta$ 1 effectors IFIT2, ISG56, OAS1 and PKR, thereby establishing that PKC $\epsilon$ /pATF2 levels repress chemotherapeutic stress-induced IFN $\beta$ 1 expression and signaling (Supplementary Figure 1f). In addition, treatment of WM793 cells with SBI-410, a small-molecule inhibitor of PKC $\epsilon$ -mediated phosphorylation of ATF2,<sup>17</sup> dose-dependently induced IFN $\beta$ 1 transcription (~2- to 9-fold; Supplementary Figure 1g). Moreover, the small interfering RNA-mediated knockdown of PKC $\epsilon$  resulted in increased expression of IFN $\beta$ 1 transcripts, both at baseline and during ETO treatment (Supplementary Figure 1h). Finally, we confirmed that ETO treatment increased IFN $\beta$ 1 protein production by ~2.5-fold in WM793 cells (Figure 1c), and to a lower degree in LU1205 (~1.8-fold) and 501Mel (~1.2-fold) cells. Similar effects were observed following CIS treatment (Figure 1c). This induction was also blocked by the expression of ATF2<sup>T52E</sup> or caPKC $\epsilon$  (Figure 1d). Together, these data indicate that the PKC $\epsilon$ –ATF2 pathway represses the stress-induced expression of IFN $\beta$ 1 and its downstream signaling effectors.

#### PKC $\epsilon$ -phosphorylated ATF2 binds the IFN $\beta$ 1 promoter to repress transcription

To determine whether pATF2 directly represses IFN $\beta$ 1 transcription in melanoma cells subjected to chemotherapeutic stress, we examined ATF2 binding to the IFN $\beta$ 1 promoter in 501Mel cells that express high levels of PKC $\epsilon$  and pATF2 and that failed to upregulate IFN $\beta$ 1 in response to stress (Supplementary Figure 1a and e). Chromatin immunoprecipitation–PCR analysis revealed high levels of the IFN $\beta$ 1 5' promoter sequence in ATF2 immunoprecipitates from cells incubated with or without ETO, suggesting that ATF2 binds constitutively to the IFN $\beta$ 1 promoter to repress transcription in cells exhibiting high levels of PKC $\epsilon$  (Figure 2a, left). In LU1205 cells that moderately upregulated IFN $\beta$ 1 following chemotherapeutic stress, chromatin immunoprecipitation analysis revealed a ~20% reduction of ATF2 binding to the IFN $\beta$ 1 promoter (Figure 2a, right), supporting the notion that the presence of ATF2 on the IFN $\beta$ 1 promoter suppresses its transcription, whereas its absence following genotoxic stress promotes it.

The IFN $\beta$ 1 5'-promoter contains four putative AP1 sites that could serve as ATF2 binding sites. To test this, we generated luciferase constructs containing varying combinations of the IFN $\beta$ 1 promoter AP1 sites (E1, E2, E3 and E4; Figure 2b), and evaluated their activity in WM793 cells coexpressing empty vector or ATF2<sup>T52E</sup>. ETO and CIS treatment induced luciferase expression ~2-fold in cells expressing the full-length construct (containing E1–E4) (Figure 2b, lower, and Figure 2c), consistent with the effects of chemotherapeutic stress on endogenous IFN $\beta$ 1. Constructs consisting of the E3 domain alone (#3) or E3+E4 domains (#4) exhibited an ~2- to 4-fold higher luciferase activity compared with cells expressing the full-length construct, in the presence or absence of ETO (Figure 2c), suggesting the presence of a transcriptional activating element. However, only the E1-containing full-length and E1–3 (#123) constructs were transcriptionally repressed by ATF2<sup>T52E</sup>, suggesting that the E1

element is required for pATF2-mediated transcriptional suppression (Figure 2d). Indeed, mutation of the AP1 consensus-binding motif in E1 abrogated the ATF2<sup>T52E</sup> transcriptional repression ( $\Delta$ E1; Figure 2e). These data indicate that pATF2 represses IFN $\beta$ 1 transcription by binding to the E1 element within the 5'-untranslated region of the IFN $\beta$ 1 gene.

#### IFN $\beta$ 1 induction results in delayed S-phase and a senescence-like phenotype

To determine the biological action of IFN $\beta$ 1 in melanoma cells, we examined two- and three-dimensional growth in WM793 cells overexpressing IFN $\beta$ 1 or 501Mel cells treated with exogenous recombinant human IFN $\beta$ 1, respectively, and found that both treatments significantly impaired melanoma cell proliferation when grown in standard tissue culture conditions as well as in three-dimensional spheroid culture (Figure 3a, left and right). Furthermore, IFN $\beta$ 1 treatment effectively doubled the proportion of LU1205 cells in the S and G2 phases of the cell cycle compared with untreated cells (Figure 3b). In addition, the number of cells in S phase was ~10% higher in cultures treated with both IFN $\beta$ 1 and ETO compared with ETO alone (Figure 3b). These data indicate that IFN $\beta$ 1 treatment promotes the accumulation of cells in S phase and is sufficient, when applied as a single agent, to double the S-phase population. We posited that this effect of IFN $\beta$ 1 might be because of activation of the intra-S-phase checkpoint. Indeed, immunostaining for the DNA repair protein Mre11 revealed that IFN $\beta$ 1 treatment increased the frequency of bulky Mre11-positive DNA repair foci by ~40% (Figure 3c), consistent with the accumulation of cells in late S phase.<sup>18</sup> These data therefore demonstrate that IFN $\beta$ 1 impairs S/G2-phase progression.

We next asked whether inhibition of IFN $\beta$ 1 signaling might reverse the cell-cycle effects of ETO. To this end, we performed short hairpin RNA-mediated knockdown of the IFN $\beta$ 1 receptor subunit IFNAR2 in WM793 cells (Supplementary Figure 2a) and assessed cell-cycle progression and viability under chemotherapeutic stress. Control cells expressing scrambled short hairpin RNA exhibited an ~30% increase in S/G2-phase cells and increased dead/dying cells following exposure to ETO (Figures 3d and e). In contrast, knockdown of IFNAR2 increased the percentage of ETO-treated cells in G1 (~15–20%), and reduced S-phase accumulation and cell death by ~10% and ~13%, respectively, compared with control ETO-treated cells (Figures 3d and e). A similar reduction of chemotherapeutic stress-induced cell death and increase in G1-phase cells was observed in cells overexpressing caPKC $\epsilon$  or ATF2<sup>T52E</sup> compared with empty vector-expressing cells (Supplementary Figure 2b), consistent with the cell-cycle changes being driven by PKC $\epsilon$ –ATF2-mediated signaling.

Interestingly, the effects of IFN $\beta$ 1 and ETO on the cell cycle were accompanied by a senescence-like phenotype characterized by the increased activity of senescence-associated  $\beta$ -galactosidase and the expression of senescence markers including DEC1, DCR2 and p21, but not p16, p53 or p27 (Figure 4a). Despite this profile, the cells treated with ETO and/or IFN $\beta$ 1 continued to proliferate, although at a greatly reduced rate (Figure 3a and data not shown). The mutant B-RAF inhibitor PLX4720 has also been shown to induce senescence-associated  $\beta$ -galactosidase activity.<sup>19</sup> In agreement, PLX4720 treatment of WM793 cells increased senescence-associated  $\beta$ -galactosidase activity (Figure 4a) and also induced the transcription of IFN $\beta$ 1 (Figure 4b), similar to the effects of ETO and CIS. These results indicate that the therapeutic stress-induced expression of IFN $\beta$ 1 in melanoma cells results in impaired S/G2 transit that is characterized by increased DNA repair foci and a senescence-like phenotype.

#### IFN $\beta$ 1 cotreatment enhances chemotherapeutic efficacy

We hypothesized that the IFN $\beta$ 1-induced S-phase accumulation might enhance the sensitivity of melanoma cells to

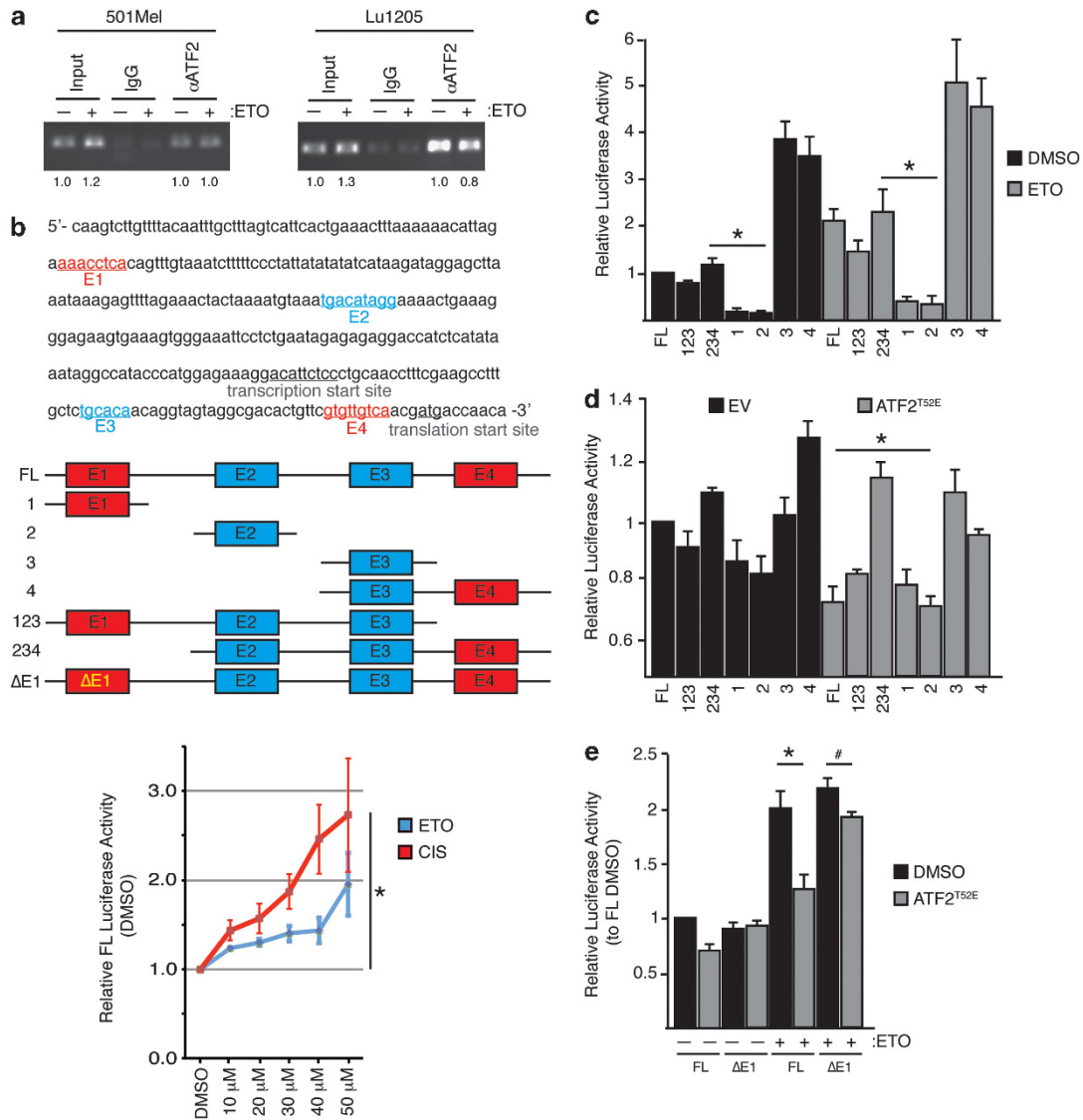


**Figure 2.** PKC $\epsilon$ -phosphorylated ATF2 binds to and represses transcription of the IFN $\beta$ 1 promoter. **(a)** Chromatin immunoprecipitation (ChIP)–PCR analysis of ATF2-associated 5'-IFN $\beta$ 1 promoter in 501Mel (left) and LU1205 (right) cells treated with dimethyl sulfoxide (DMSO) or 10  $\mu$ M etoposide (ETO) for 24 h. **(b, upper)** Schematic of the 5'-untranslated region (UTR) of the human IFN $\beta$ 1 gene showing E2 and E3 AP1 sites on the forward strand and E1 and E4 AP1 sites on the reverse strand. **(b, middle)** IFN $\beta$ 1 promoter luciferase constructs are shown below.  $\Delta$ E1 contains a mutagenized E1 site. **(b, lower)** Quantitation of full-length (FL) IFN $\beta$ 1 promoter luciferase construct activity upon treatment with DMSO, ETO or 10  $\mu$ M CIS for 24 h at the indicated concentrations. \* $P$  < 0.001. **(c)** Luciferase assays of WM793 cells expressing the indicated IFN $\beta$ 1 promoter luciferase constructs and treated with DMSO or ETO overnight. Results are expressed relative to the luciferase activity in cells expressing the DMSO-treated FL construct. \* $P$  < 0.0005. **(d)** Luciferase assays performed as in (c) on WM793 cells co-transfected with the IFN $\beta$ 1 promoter luciferase constructs and either empty vector (EV) or ATF2<sup>T52E</sup>. \* $P$  = 0.0005. **(e)** Luciferase assays performed as in (c) with WM793 cells co-transfected with the indicated IFN $\beta$ 1 promoter luciferase constructs and either EV or ATF2<sup>T52E</sup> and treated with DMSO or ETO. \* $P$  = 0.0018; # $P$  = 0.03. The results shown represent the mean values  $\pm$  s.d. of experiments performed in biological triplicate.

chemotherapeutic agents or PLX4720. Indeed, we found that whereas treatment with IFN $\beta$ 1 alone was not significantly cytotoxic, the toxicity of ETO (by  $\sim$ 30%) and PLX4720 (by  $\sim$ 40%) was significantly enhanced by cotreatment with IFN $\beta$ 1 (Figure 4c and Supplementary Figures 2c and d). These results suggest that the cell cycle-altering effects of IFN $\beta$ 1 can sensitize melanoma cells to chemotherapeutic agents as well as to PLX4720. In support of this notion, whereas the overexpression of caPKC $\epsilon$  or ATF2<sup>T52E</sup> suppressed ETO-induced cell death to  $\sim$ 13% or 10%, respectively, compared with  $\sim$ 27% cell death in EV-expressing cells, the co-overexpression of IFN $\beta$ 1 was sufficient to significantly overcome caPKC $\epsilon$ - or ATF2<sup>T52E</sup>-mediated resistance to ETO, restoring cell death induction to  $\sim$ 35% (Figure 4d).

Taken together, these results indicate that IFN $\beta$ 1 signaling status contributes to the responsiveness of melanoma cells to stress via intact IFN $\beta$ 1 signaling, which sensitizes cells to stress, whereas loss of IFN $\beta$ 1 signaling under stress conditions is protective. These findings support a tumor suppressor role for cell-autonomous IFN $\beta$ 1 signaling in melanoma cells—consistent with the previously observed function of PKC $\epsilon$ -phosphorylated ATF2.

Effects of chemotherapeutic stress-induced IFN $\beta$ 1 expression in melanoma cells are cell autonomous

We next asked whether chemotherapeutic stress-induced IFN $\beta$ 1 expression in melanoma cells might also elicit cell nonautonomous effects, such as immune cell-mediated tumor clearance.

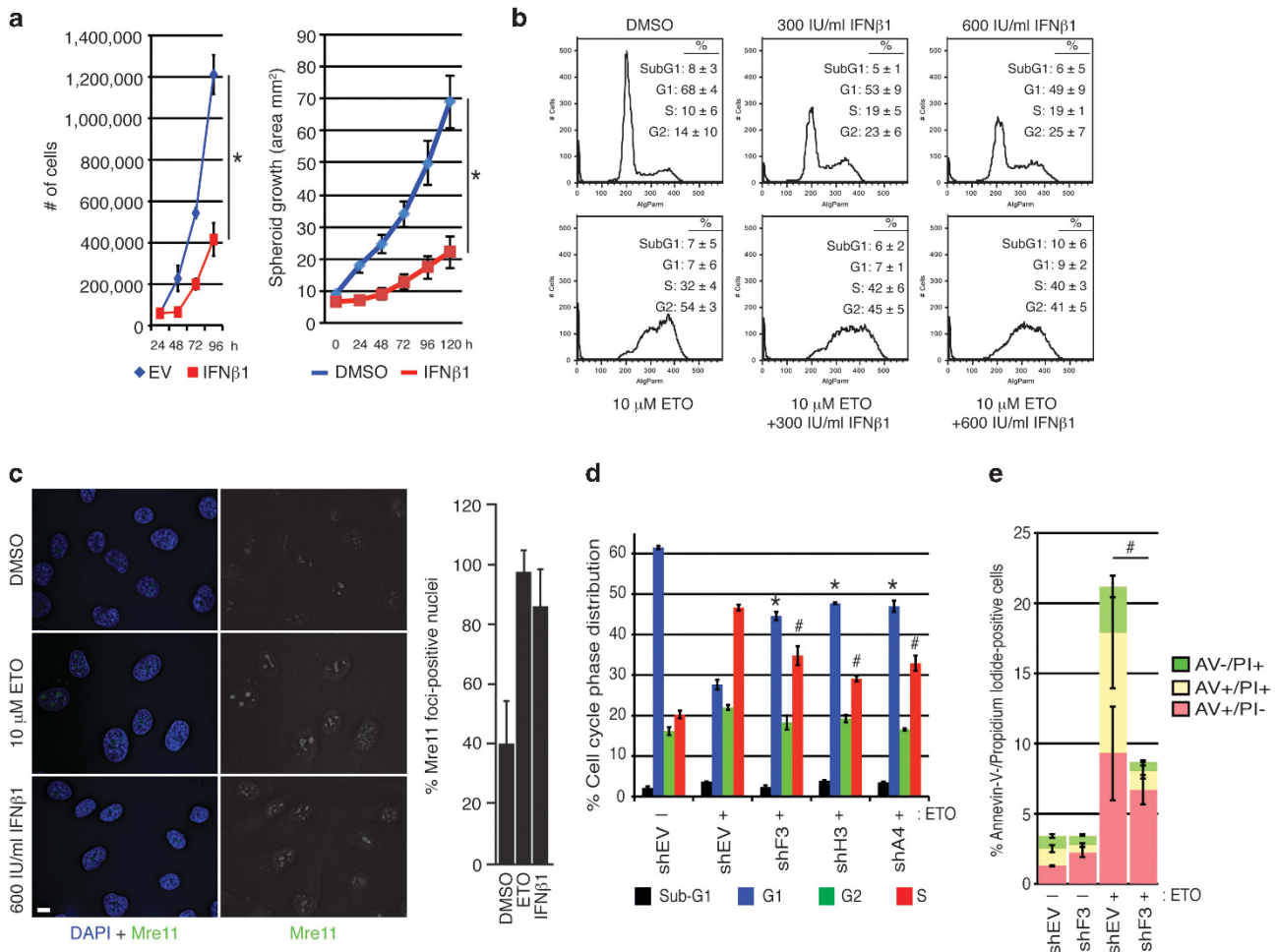


**Figure 3.** IFN $\beta$ 1 signaling impairs melanoma growth and proliferation and slows S/G2 transit. **(a, left)** Growth of WM793 cells was measured at indicated times after transfection with empty vector (EV) or vector encoding IFN $\beta$ 1. **(a, right)** The three-dimensional growth of 501Mel spheroids was measured at the indicated times after transfer to soft agar and addition of dimethyl sulfoxide (DMSO) or 300 IU/ml human IFN $\beta$ 1. Media and fresh IFN $\beta$ 1 was replenished after 72 h. \* $P < 0.0001$ . **(b)** Cell-cycle fluorescence-activated cell sorting (FACS) profiles of LU1205 cells treated as indicated for 24 h. **(c, left)** Immunofluorescent staining for Mre11 in WM793 cells treated as indicated for 24 h. DNA was stained with 4',6-diamidino-2-phenylindole (DAPI). Scale bar = 10  $\mu$ m. **(c, right)** Quantification of nuclei containing Mre11+ foci. Results are the mean values  $\pm$  s.d. of 50 nuclei per sample. **(d)** Cell cycle-phase distribution of LU1205 cells infected with EV (shEV) or short hairpin RNAs (shRNAs) targeting IFNAR1 (shA4 and shH3) or IFNAR2 (shF3). Cells were incubated with DMSO or 10  $\mu$ M etoposide (ETO) for 24 h. Cell-cycle analysis was performed as in **(b)**. \* $P < 0.0001$ ; # $P < 0.001$  compared with shEV+ETO. **(e)** Quantitation of Annexin-V and propidium iodide staining of LU1205 cells treated as indicated for 32 h. For all FACS,  $N = 10\,000$  cells per sample, and the results shown represent the mean values  $\pm$  s.d. of experiments performed in biological triplicate.

To test this, we performed co-culture experiments using the B6-derived murine Pten:Brf:Cdkn2a mutant melanoma cell line YUMM1.3<sup>20</sup> and splenic lymphocytes from syngeneic wild-type B6 mice carrying YUMM1.3 tumors. The YUMM1.3 cells were modified to express green fluorescent protein (GFP) and ATF2<sup>T34E</sup> (murine ATF2<sup>T52E</sup> equivalent) or empty vector, allowing direct assessment of the contribution of pATF2 (Figure 5a).

Treatment of YUMM1.3 cells with ionizing irradiation (IR; 5 or 10 Gy for 24 h) alone, a therapeutic stress that can be targeted specifically to the melanoma cells but not to the lymphocytes, effectively reduced cell viability by ~40%. The addition of a neutralizing anti-IFN $\beta$ 1 antibody attenuated cell death (~25% increased viability) in cells exposed to 5 Gy IR, and to a lesser extent, after 10 Gy IR, indicating that IR-induced death was partially dependent on IFN $\beta$ 1 (Figures 5a and b and Supplementary Figure 3). Although the addition of lymphocytes decreased (~20%) the viability of nonirradiated YUMM1.3 cells, the lymphocytes did not significantly reduce the viability of irradiated YUMM1.3 cells compared with irradiated YUMM1.3 cells

alone. Furthermore, the addition of an anti-IFN $\beta$ 1 antibody to these co-cultures did not affect cell viability compared with YUMM1.3 cells cultured in the absence of lymphocytes. Intriguingly, the addition of lymphocytes to cultures of ATF2<sup>T34E</sup>-expressing YUMM1.3 cells, which were refractory to irradiation, did not decrease cell viability (Figures 5a and b and Supplementary Figure 3). These results demonstrate that the IR-induced expression of IFN $\beta$ 1 in the melanoma cells elicited minimal additional effects in triggering lymphocyte-mediated tumor cell death in our co-culture system. Furthermore, flow cytometric analysis of the co-cultures revealed that the irradiated YUMM1.3 cells did not further activate CD4<sup>+</sup> or CD8<sup>+</sup> T cells, NKp46<sup>+</sup> NK cells or GR-1<sup>+</sup> lymphocytes (Supplementary Figures 4a–d) compared with nonirradiated cells, whereas the neutralizing IFN $\beta$ 1 antibody abolished their basal activation state (Supplementary Figure 4).

Together, these data indicate that the changes observed in melanoma cells following altered IFN $\beta$ 1 expression are predominantly because of cell-autonomous effects.

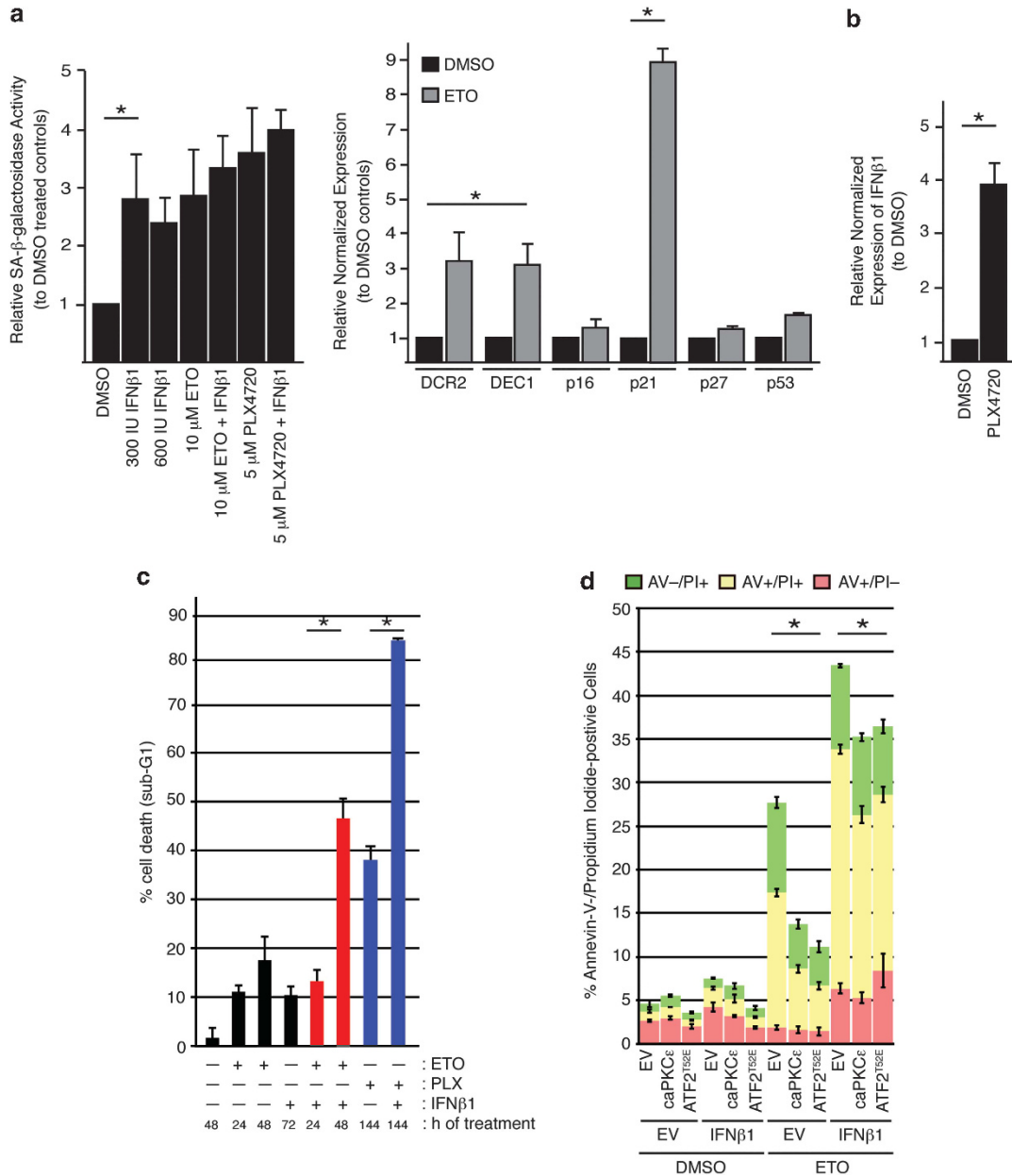


**Figure 4.** IFNβ1 induces a senescence-like phenotype and enhances the toxicity of etoposide and PLX4720. **(a, left panel)** Senescence-associated β-galactosidase (SA-β-gal) activity in WM793 cells treated as indicated overnight. **(a, right panel)** Quantitative real-time reverse transcription-PCR (qRT-PCR) analysis of DCR2, DEC1 and p16 transcripts in WM793 cells treated with dimethyl sulfoxide (DMSO) or 10 μM ETO overnight. \**P* < 0.05. **(b)** qRT-PCR analysis of IFNβ1 transcripts in WM793 cells treated with DMSO or 5 μM PLX4720 overnight. For **(a, b)**, results represent the mean values ± s.d. of triplicates and are expressed relative to cells treated with DMSO. **(c)** Quantification of dead cell (sub-G1) population of WM793 cells treated with 600 IU/ml human IFNβ1 (6 h of pretreatment) ± 10 μM ETO or 5 μM PLX4720 (PLX) and analyzed by flow cytometry at the indicated times. #*P* < 0.005. **(d)** Quantitation of Annexin-V and propidium iodide staining of empty vector (EV) and WM793 cells co-overexpressing EV or IFNβ1 that were incubated in the presence of DMSO or ETO for 32 h.

Subcellular localization of ATF2 and expression of IFNβ1 in human melanomas correlates with therapeutic responsiveness

We next investigated whether ATF2 and IFNβ1 status in melanoma tumors might associate with clinical outcome. We hypothesized that after treatment, tumors exhibiting cytoplasmic accumulation of ATF2 and induction of IFNβ1 would correlate with therapeutic responsiveness, whereas those exhibiting nuclear enrichment of ATF2 and no induction or reduction of IFNβ1 would correlate with nonresponsiveness to therapy. To this end, we examined pre- and post-treatment melanoma tumor samples obtained from three medical centers.

The first cohort of patients specimens assessed were paired pre- and post-treatment melanoma tumor sections obtained from elective surgeries on 9 AJCC (American Joint Committee on Cancer) stage IIIc/IV cutaneous melanoma patients who were administered combinatorial biochemotherapy (cisplatin, dacarbazine, vinblastine, IL-2 and IFN-α2a),<sup>21,22</sup> dacarbazine, temodar, and/or had radiation (gamma knife) with several years of follow-up (John Wayne Cancer Institute, Santa Monica, CA, USA). ATF2 localization (nuclear vs cytoplasmic) and IFNβ1 levels were examined and compared, by blinded analysis, between the patient-matched pre- and post-treatment tissue sections by

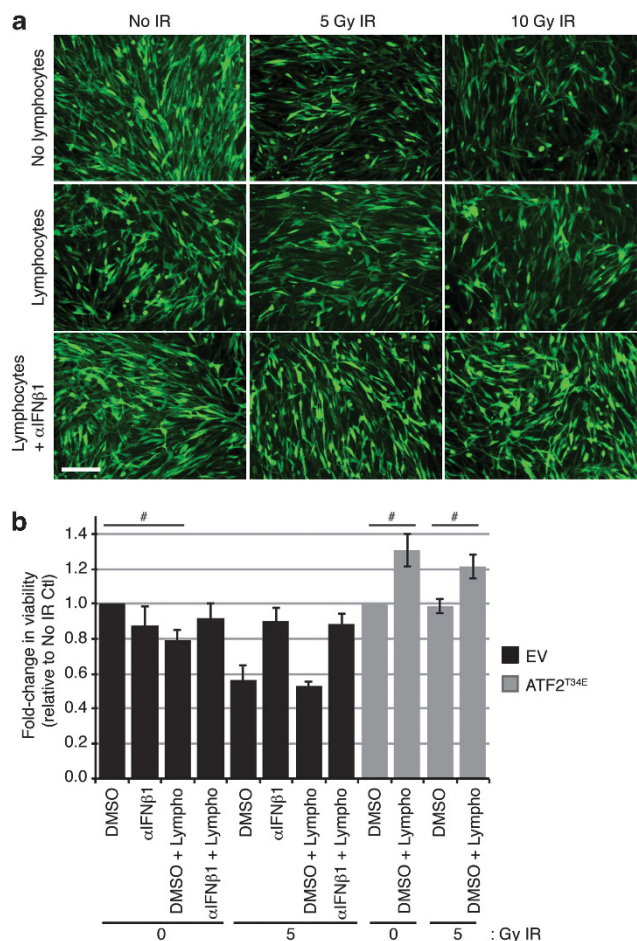


**Figure 5.** Chemotherapeutic stress-induced expression of IFN $\beta$ 1 in melanoma cells does not activate lymphocytes to mediate tumor clearance. **(a)** Immunofluorescence images of green fluorescent protein (GFP)-expressing YUMM1.3 (B6 syngeneic) murine melanoma cells, either untreated or exposed to 5 Gy IR and cultured for 24 h with or without lymphocytes (melanoma to lymphocyte ratio: 1:30) from the spleens of B6 mice that were previously inoculated subcutaneously with YUMM1.3 tumors (for 1 month). Anti-IFN $\beta$ 1 antibody ( $\alpha$ IFN $\beta$ 1) was added at 10  $\mu$ g/ml as indicated. Images were acquired after 24 h of culture. Scale bar = 100  $\mu$ m. **(b)** Viability of GFP-expressing YUMM1.3 cells co-transfected with empty vector (EV) or vector encoding ATF2<sup>T34E</sup> and treated as in **(a)**. Viability was measured as described in the Materials and methods section after 24 h of culture. The results represent the mean values  $\pm$  s.d. of triplicates. <sup>#</sup>*P* < 0.005.

immunofluorescence microscopy and were found to correlate with clinical responsiveness (time to progression) for 7 of the 9 patients assessed as follows: 3 of 3 patients exhibiting poor responses and 4 of 6 patients exhibiting favorable responses (Supplementary Figures 5a and b and 6a). Furthermore, a separate cohort of 8 nontreated melanoma patient specimens and 15 drug-treated nonresponder specimens (from patients who had progressed/recurred rapidly on treatment) demonstrated a ninefold reduction in IFN $\beta$ 1 expression, as determined by qRT-PCR analysis, consistent with the transcriptional repression of IFN $\beta$ 1 in nonresponsive patients (Supplementary Figure 6c). Drug therapies for the treated patients included ipilimumab, MEK inhibitor, vemurafenib, IFN- $\alpha$ 2a, abraxane and/or avastin.

As pATF2 was associated with downregulated IFN $\beta$ 1 and its downstream effectors, we assessed the possibility that the status of ATF2 and IFN $\beta$ 1 might correlate with responsiveness to IFN-based therapy. Thus, we examined pre- and post-treatment

tumor sections from an independent cohort of 12 melanoma patients who were administered single-agent neoadjuvant IFN- $\alpha$ 2a (University of Pittsburgh Cancer Institute Melanoma Center). Blinded scoring and comparison of the patient-matched sections for changes in ATF2 localization and IFN $\beta$ 1 expression before and after treatment revealed a strong association with clinical responsiveness (time to progression) in 8 of 12 patients: 3 of 4 patients exhibited poor responses and 5 of 8 patients exhibited favorable responses (Figures 6a and b and Supplementary Figure 6b). Consistent with these findings, analyses of pre- and post-IFN- $\alpha$ 2a-treated tumor samples from five nonresponder patients (from the University of Zurich) revealed unchanged or reduced IFN $\beta$ 1 and nuclear ATF2 staining (Supplementary Figure 8).

CD8+ T-cell infiltration and intratumoral proliferation represents an important component of antitumor immunity,<sup>23</sup> and thus we examined whether the samples from the biochemotherapy and IFN- $\alpha$ 2a patient cohorts exhibited a correlation between the presence of CD8+ T cells, patient responsiveness and ATF2/IFN $\beta$ 1 status. In this analysis, we hypothesized that the presence of CD8+ T cells after treatment would correlate with responsiveness, whereas lack of CD8+ T cells would correlate with nonresponsiveness. By immunofluorescence assessment of the biochemotherapy cohort samples, we found that 5 of 9 patients exhibited increased CD8+ T-cell populations in responders but not in nonresponders (Figures 6c and d and Supplementary Figures 6a and b). In the IFN- $\alpha$ 2a cohort, 6 of 12 patients exhibited increased CD8+ T-cell populations in responders but not in nonresponders (Figures 6c and d and Supplementary Figures 6a and b). Notably, in both cohorts, the patients who exhibited a correlation of CD8+ T-cell populations with responsiveness or nonresponsiveness were also patients whose responses also correlated with ATF2 and IFN $\beta$ 1 status. These observations suggest that although the therapeutic stress-induced expression of IFN $\beta$ 1 that we observe in melanoma cells is insufficient to trigger lymphocyte activation/infiltration, it does not preclude the presence/proliferation of intratumoral CD8+ T-cell populations that are likely affected by mechanisms that are independent of the therapy-induced, ATF2-regulated expression of IFN $\beta$ 1.

Taken together, the analyses of patient samples support our mechanistic data, indicating that the transcriptional repression of IFN $\beta$ 1 expression by PKC $\epsilon$ -ATF2 drives melanoma resistance. In addition, we also assessed the status of ATF2 and IFN $\beta$ 1 in a cohort of 17 melanoma patients who were treated with IL-2 at the Anschutz Medical Campus of the University of Colorado, and we did not observe a significant correlation between these proteins and patient responsiveness (data not shown), suggesting that this mechanism of resistance might apply to specific therapeutic modalities. Nonetheless, in the other treatment cohorts, we find that the profile of ATF2 localization and IFN $\beta$ 1 expression appears to correlate with clinical responsiveness (time to progression) in ~70% of the patients examined; additional independent larger-cohort studies are required to further substantiate these observations.

## DISCUSSION

The development of resistance to advanced and specific therapies represents a continuing challenge for effective and durable treatment responses of melanoma. Improving our understanding of the crucial mechanisms that propel resistance in melanoma will aid in the improvement and development of current and future therapeutic modalities as well as potentially patient stratification that would represent a major advance for the treatment of melanoma. Here, we report a previously undisclosed molecular mechanism that facilitates the development of the resistance of melanoma to therapeutic stress.

Our data demonstrate that PKC $\epsilon$ -phosphorylated ATF2 down-regulates IFN $\beta$ 1 expression (and signaling) that promotes the

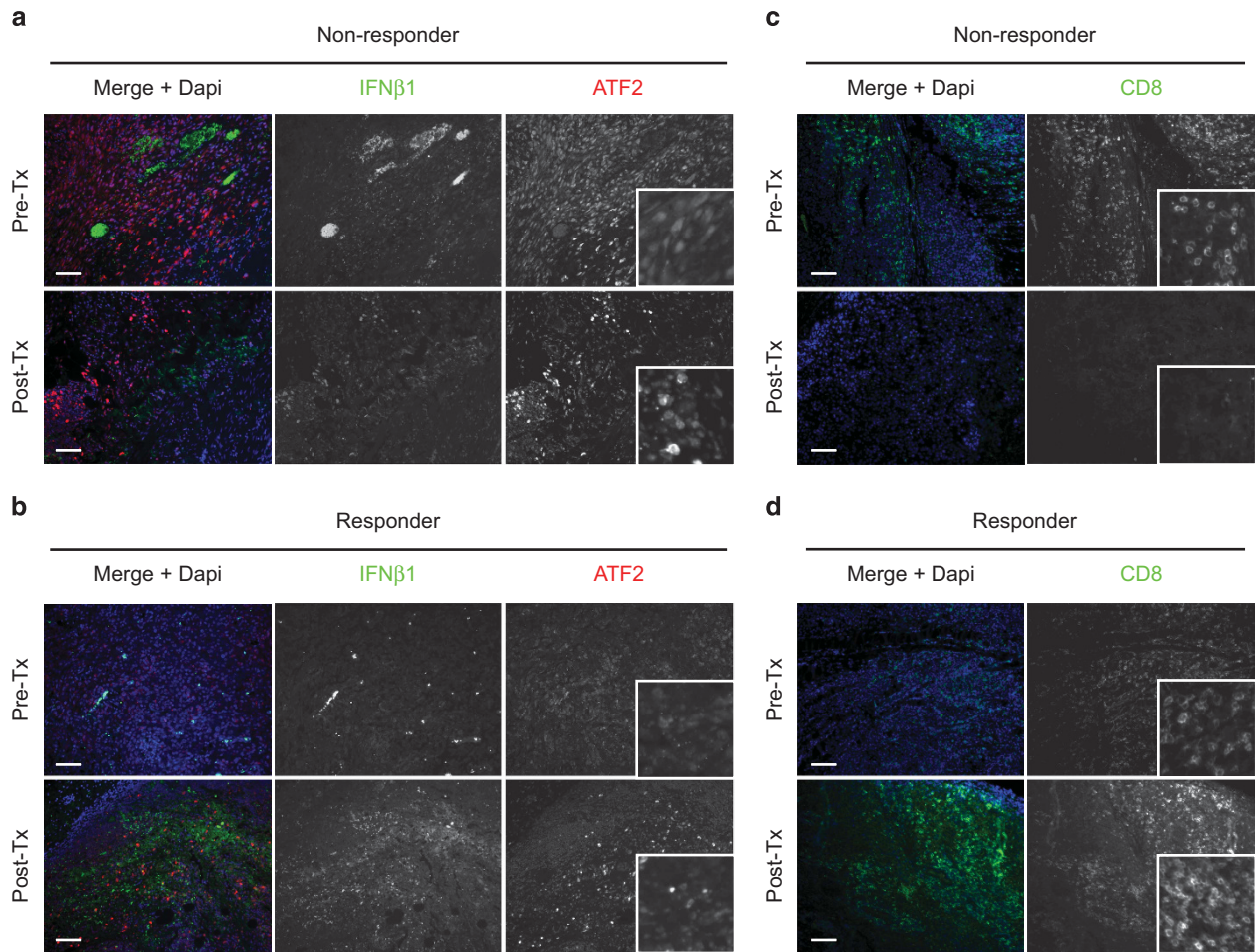


**Figure 6.** IFN $\beta$ 1 expression, ATF2 subcellular localization and the presence of CD8+ T cells in melanoma patient tumor samples correlates with therapeutic responsiveness. Immunofluorescence staining for ATF2 (red) and IFN $\beta$ 1 (green) in representative melanoma tumor sections from a responder (a) and nonresponder (b) patient from the University of Pittsburgh Cancer Center (UPCC) cohort, before (Pre-Tx; upper) and after (Post-Tx; lower) IFN- $\alpha$ 2a treatment as indicated in the text, is shown. Immunofluorescence staining for CD8 in representative sections from a nonresponder (c) or responder (d) patient from the John Wayne Cancer Institute (JWCI) cohort, before (Pre-Tx; upper) and after (Post-Tx; lower) biochemotherapy treatment as indicated in the text, is shown. Nuclei were counterstained with 4',6-diamidino-2-phenylindole (DAPI). Scale bars represent 100  $\mu$ m.

resistance of melanoma cells to chemotherapeutic agents, as well as the BRAF inhibitor PLX4720 (the model compound for PLX4032/vemurafenib). Phosphorylated ATF2 directly represses IFN $\beta$ 1 transcription, and attenuating ATF2-mediated suppression enables the induction of IFN $\beta$ 1 and its tumor-suppressive effects. We found that the stress-induced expression of IFN $\beta$ 1 elicits predominantly cell-autonomous effects on melanoma cells—which might be explained by the fact that chemotherapy induces  $\sim$ 2.5-fold increases in IFN $\beta$ 1 protein levels, whereas infectious stimuli (that is, viral infection or lipopolysaccharide exposure) that elicit immune responses have been reported to induce IFN $\beta$ 1 to levels on the order of thousands of fold increase.<sup>24–26</sup> The chemotherapy-induced IFN $\beta$ 1 impairs growth and proliferation by altering cell-cycle dynamics and inducing the accumulation of cells in S/G2 phases and sensitizing melanoma cells to death.

Melanomas are notorious for their propensity for developing resistance to a range of therapies, including DNA-damaging agents.<sup>10,27–29</sup> We found that the upregulation of PKC $\epsilon$ -ATF2 signaling and subsequent repression of IFN $\beta$ 1 in cells exposed to chemotherapeutic stress is sufficient to alter cell-cycle dynamics and to reduce the population of cells in S phase, identifying one mechanism by which melanomas develop resistance to chemotherapeutic agents. Indeed, the expression of constitutively

active PKC $\epsilon$  or pATF2 renders melanoma cells with low endogenous levels of PKC $\epsilon$ /pATF2 less responsive to the cytotoxic effects of exogenous IFN $\beta$ 1 and/or ETO (Supplementary Figure 7). It is possible that, by driving the nuclear localization and activity of ATF2, PKC $\epsilon$  might also promote the DNA repair function of ATF2,<sup>30</sup> further contributing to enhanced melanoma survival during therapeutic stress—a point that deserves further investigation. That PKC $\epsilon$ -ATF2 reduced IFN $\beta$ 1/ETO responsiveness (measured by cell death) by only  $\sim$ 50% suggests that other downstream ATF2-dependent and ATF2-independent mechanisms also contribute to the development of therapeutic resistance. Of note, the correlation of intratumoral CD8+ T-cell populations, ATF2/IFN $\beta$ 1 status and patient responsiveness that we observed in the biochemotherapy cohort samples, but not in our co-culture studies, implies an effect of PKC $\epsilon$ -ATF2 on the proliferation of intratumoral CD8+ T cells rather than the recruitment of CD8+ T cells. Further studies on how ATF2 modulates intratumoral immune responses are warranted.

Our findings are corroborated by the analyses of samples from melanoma patients before and after biochemotherapy/chemotherapy/radiation treatment, as well as neoadjuvant IFN- $\alpha$ 2a therapy. Accordingly, tumors from patients classified as therapeutic responders exhibited increased levels of cytoplasmic (transcriptionally inert) ATF2 and correspondingly increased IFN $\beta$ 1



levels. Conversely, nonresponders exhibited nuclear ATF2 and unaltered or reduced levels of IFN $\beta$ 1 after treatment. These findings therefore offer mechanistic insight into the development of therapeutic resistance through downregulation of a mitogen-activated protein kinase pathway-independent molecular mechanism that would otherwise sensitize tumor cells to chemotherapeutic/therapeutic stress. Such alterations correlated with the clinical responsiveness of the majority of patients we evaluated, suggesting that PKC $\epsilon$ -ATF2-IFN $\beta$ 1 signaling plays an important role in melanoma resistance and progression in patients. Further, our data suggest that ATF2 and IFN $\beta$ 1 might represent novel markers of clinical responsiveness, a possibility that requires further assessment in large cohort studies. Findings from recent clinical studies support the possibility that the mechanism (and ATF2/IFN $\beta$ 1 profile) that we have identified extends beyond melanoma to other types of cancers. For example, the expression of type-1 IFNs (including IFN $\beta$ 1) was recently found to correlate with biochemical recurrence and metastasis in prostate and breast cancer patients, respectively, although the underlying mechanism was unclear in those studies.<sup>31,32</sup> Furthermore, recent *in vitro* studies suggest that tumor stroma-derived IFN $\beta$ 1, such as that from adipose tissue, also elicits tumor-suppressive effects,<sup>33</sup> and the treatment of other cancer cell types, including hepatocellular carcinoma cells, with IFN $\beta$ 1, was recently found to elicit similar cell-cycle alterations and cell death as those identified in our study.<sup>34,35</sup>

Importantly, the results of this study also suggest the potential therapeutic value of agents that can promote ATF2 cytoplasmic localization, thereby derepressing IFN $\beta$ 1 transcription. We previously showed that the inhibition of PKC $\epsilon$ -mediated phosphorylation of ATF2 promotes its accumulation at the mitochondrial outer membrane, where it contributes to stress-induced mitochondrial leakage.<sup>14</sup> Our subsequent high-content microscopy-based screen identified two compounds that trigger the cytoplasmic/mitochondrial localization of ATF2, simultaneously blocking its transcriptional activity.<sup>17</sup> Of those, SBI-0089410 effectively induced the expression of IFN $\beta$ 1 (Supplementary Figure 1g), supporting the possibility that such compounds could enhance the chemosensitivity of melanoma cells by both promoting the mitochondrial function of ATF2 and simultaneously derepressing IFN $\beta$ 1 signaling.

In conclusion, our study has identified a molecular mechanism that underlies the oncogenic function of ATF2, as reflected in its ability to drive chemoresistance of melanomas. PKC $\epsilon$ , which we previously found to be upregulated in metastatic melanoma,<sup>14</sup> and which is one of the top 10 kinases that can confer resistance in melanoma to mutant BRAF inhibition,<sup>2</sup> phosphorylates ATF2 and triggers the downregulation of IFN $\beta$ 1 signaling that we have now shown determines the therapeutic responsiveness of melanoma cells by modulating cell-cycle dynamics and sensitivity to stress induced by chemotherapeutic therapeutic agents. Notably, the recent finding that ATF2 mediates sorafenib resistance in liver cancer suggests that the mechanism of therapeutic resistance that we have uncovered might represent a mode of resistance that pertains to other types of cancers beyond melanoma.

## MATERIALS AND METHODS

### Cell lines

All cell lines were maintained in Dulbecco's modified Eagle's medium supplemented with 10% fetal bovine serum and antibiotics.

### Antibodies and immunostaining reagents

Antibodies employed were purchased as follows: ATF2 (C-19 for immunoblotting and C-19X for chromatin immunoprecipitation assays) and PKC $\epsilon$  (C15), IFN $\beta$ 1 (E-20, for immunostaining of sections) from Santa

Cruz Biotechnology, Inc. (Santa Cruz, CA, USA); IFN $\beta$ 1 (AP18065PU-N, for intracellular fluorescence-activated cell sorting and immunoneutralization assays) from Acris (San Diego, CA, USA);  $\beta$ -tubulin (E7-s) from Developmental Studies Hybridoma Bank (University of Iowa, Iowa city, IA, USA); and pT52-ATF2 (Phosphosolutions, Aurora, CO, USA). For immunofluorescent staining of ATF2 in patient sections, we used a polyclonal antibody made by SDIX, LLC (Newark, DE, USA) against the amino-acid residues 129–278.

### DNA constructs and transfection

DNA plasmids were all transfected using JetPrime (Polyplus, Illkirch, France) or Lipofectamine 2000 (Invitrogen, Carlsbad, CA, USA) according to the manufacturers' protocols. The constitutively active HIS-tagged PKC $\epsilon$  construct was a generous gift from Dr Jorge Moscat (Sanford-Burnham Medical Research Institute, La Jolla, CA, USA). Other plasmids have been previously described.<sup>14</sup>

### Flow cytometric analyses

**Cell-cycle analysis.** Cells were seeded at  $1 \times 10^5$  cells per well into 6-well tissue culture plates and treated the next day as indicated in the figure legend. Following treatment, cells were harvested by trypsinization and fixed in 70% EtOH in phosphate-buffered saline. After a single wash in phosphate-buffered saline, the cells were stained in cell cycle staining buffer (60  $\mu$ g/ml propidium iodide/0.15 mg/ml RNase A (Sigma, St Louis, MO, USA)). After incubation for 20 min, the cells were immediately analyzed by fluorescence-activated cell sorting,  $n = 10\,000$  cells (within G1 to G2 gates) per replicate over 3 independent experiments. The fluorescence activated cell sorting data were subsequently analyzed using FlowJo software (TreeStar, Ashland, OR, USA).

**Cell death analyses.** Cells were seeded at  $1 \times 10^5$  cells per well into 6-well tissue culture plates and treated the next day as indicated in the figure legend. After treatment, the cells were harvested and stained using the BioVision Annexin-V-FITC Apoptosis Detection Kit (BioVision, Milpitas, CA, USA),  $n = 10\,000$  cells (within whole cell FSC:SSC gates) per replicate over 3 independent experiments. The fluorescence-activated cell sorting data were subsequently analyzed using FlowJo software (TreeStar).

## CONFLICT OF INTEREST

The authors declare no conflict of interest.

## ACKNOWLEDGEMENTS

We thank Serge Fuchs (UPENN) and members of the Ronai laboratory for crucial scientific discussions and critical reading of this manuscript. Additional thanks to Mitch Levesque and Valerie Amann for their assistance in providing patient samples from the Department of Dermatology, University of Zurich. We are grateful to Jian-Liang Li of the SBMRI Bioinformatics Core, as well as the SBMRI Flow Cytometry and Histology Core, for technical support. Support from NCI P01 (CA128814), R01 (CA179170), Hervey Family Non-endowment Fund at The San Diego Foundation and a Melanoma Research Foundation grant to ZAR are gratefully acknowledged. Support from NCI Grants R01 (CA164679) and P01 (CA177322) to CW and P50 SPORE (CA121973) to JMK is also gratefully acknowledged. EL has been supported by K99 (CA172705) and T32 (CA121949) Grants.

## REFERENCES

- 1 Sun C, Wang L, Huang S, Heynen GJ, Prahallad A, Robert C *et al*. Reversible and adaptive resistance to BRAF(V600E) inhibition in melanoma. *Nature* 2014; **508**: 118–122.
- 2 Johannessen CM, Boehm JS, Kim SY, Thomas SR, Wardwell L, Johnson LA *et al*. COT drives resistance to RAF inhibition through MAP kinase pathway reactivation. *Nature* 2010; **468**: 968–972.
- 3 Nazarian R, Shi H, Wang Q, Kong X, Koya RC, Lee H *et al*. Melanomas acquire resistance to B-RAF(V600E) inhibition by RTK or N-RAS upregulation. *Nature* 2010; **468**: 973–977.
- 4 Van Allen EM, Wagle N, Sucker A, Treacy DJ, Johannessen CM, Goetz EM *et al*. The genetic landscape of clinical resistance to RAF inhibition in metastatic melanoma. *Cancer Discov* 2014; **4**: 94–109.

- 5 Hodi FS, O'Day SJ, McDermott DF, Weber RW, Sosman JA, Haanen JB *et al*. Improved survival with ipilimumab in patients with metastatic melanoma. *N Engl J Med* 2010; **363**: 711–723.
- 6 Robert C, Thomas L, Bondarenko I, O'Day S, Weber J, Garbe C *et al*. Ipilimumab plus dacarbazine for previously untreated metastatic melanoma. *N Engl J Med* 2011; **364**: 2517–2526.
- 7 Topalian SL, Sznol M, McDermott DF, Kluger HM, Carvajal RD, Sharfman WH *et al*. Survival, durable tumor remission, and long-term safety in patients with advanced melanoma receiving nivolumab. *J Clin Oncol* 2014; **32**: 1020–1030.
- 8 Hamid O, Robert C, Daud A, Hodi FS, Hwu WJ, Kefford R *et al*. Safety and tumor responses with lambrolizumab (anti-PD-1) in melanoma. *N Engl J Med* 2013; **369**: 134–144.
- 9 Topalian SL, Hodi FS, Brahmer JR, Gettinger SN, Smith DC, McDermott DF *et al*. Safety, activity, and immune correlates of anti-PD-1 antibody in cancer. *N Engl J Med* 2012; **366**: 2443–2454.
- 10 Ives NJ, Stowe RL, Lorigan P, Wheatley K. Chemotherapy compared with biochemotherapy for the treatment of metastatic melanoma: a meta-analysis of 18 trials involving 2,621 patients. *J Clin Oncol* 2007; **25**: 5426–5434.
- 11 Garbe C, Eigentler TK, Keilholz U, Hauschild A, Kirkwood JM. Systematic review of medical treatment in melanoma: current status and future prospects. *Oncologist* 2011; **16**: 5–24.
- 12 Rubin KM. Management of primary cutaneous and metastatic melanoma. *Semin Oncol Nurs* 2013; **29**: 195–205.
- 13 Schuchter LM. Adjuvant interferon therapy for melanoma: high-dose, low-dose, no dose, which dose? *J Clin Oncol* 2004; **22**: 7–10.
- 14 Lau E, Kluger H, Varsano T, Lee K, Scheffler I, Rimm DL *et al*. PKCepsilon promotes oncogenic functions of ATF2 in the nucleus while blocking its apoptotic function at mitochondria. *Cell* 2012; **148**: 543–555.
- 15 Rudalska R, Dauch D, Longrich T, McJunkin K, Wuestefeld T, Kang TW *et al*. In vivo RNAi screening identifies a mechanism of sorafenib resistance in liver cancer. *Nat Med* 2014; **20**: 1138–1146.
- 16 Bhoumik A, Jones N, Ronai Z. Transcriptional switch by activating transcription factor 2-derived peptide sensitizes melanoma cells to apoptosis and inhibits their tumorigenicity. *Proc Natl Acad Sci USA* 2004; **101**: 4222–4227.
- 17 Varsano T, Lau E, Feng Y, Garrido M, Milan L, Heynen-Genel S *et al*. Inhibition of melanoma growth by small molecules that promote the mitochondrial localization of ATF2. *Clin Cancer Res* 2013; **19**: 2710–2722.
- 18 Mirzoeva OK, Petrini JH. DNA replication-dependent nuclear dynamics of the Mre11 complex. *Mol Cancer Res* 2003; **1**: 207–218.
- 19 Haferkamp S, Borst A, Adam C, Becker TM, Motschenbacher S, Windhovel S *et al*. Vemurafenib induces senescence features in melanoma cells. *J Invest Dermatol* 2013; **133**: 1601–1609.
- 20 Pencheva N, Buss CG, Posada J, Merghoub T, Tavazoie SF. Broad-spectrum therapeutic suppression of metastatic melanoma through nuclear hormone receptor activation. *Cell* 2014; **156**: 986–1001.
- 21 Koyanagi K, O'Day SJ, Gonzalez R, Lewis K, Robinson WA, Amatruda TT *et al*. Serial monitoring of circulating melanoma cells during neoadjuvant biochemotherapy for stage III melanoma: outcome prediction in a multicenter trial. *J Clin Oncol* 2005; **23**: 8057–8064.
- 22 Koyanagi K, O'Day SJ, Boasberg P, Atkins MB, Wang HJ, Gonzalez R *et al*. Serial monitoring of circulating tumor cells predicts outcome of induction biochemotherapy plus maintenance biotherapy for metastatic melanoma. *Clin Cancer Res* 2010; **16**: 2402–2408.
- 23 Gajewski TF, Fuertes MB, Woo SR. Innate immune sensing of cancer: clues from an identified role for type I IFNs. *Cancer Immunol Immunother* 2012; **61**: 1343–1347.
- 24 Jacobs AT, Ignarro LJ. Lipopolysaccharide-induced expression of interferon-beta mediates the timing of inducible nitric-oxide synthase induction in RAW 264.7 macrophages. *J Biol Chem* 2001; **276**: 47950–47957.
- 25 Malmgaard L, Salazar-Mather TP, Lewis CA, Biron CA. Promotion of alpha/beta interferon induction during in vivo viral infection through alpha/beta interferon receptor/STAT1 system-dependent and -independent pathways. *J Virol* 2002; **76**: 4520–4525.
- 26 Wang J, Basagoudanavar SH, Wang X, Hopewell E, Albrecht R, Garcia-Sastre A *et al*. NF-kappa B RelA subunit is crucial for early IFN-beta expression and resistance to RNA virus replication. *J Immunol* 2010; **185**: 1720–1729.
- 27 Middleton MR, Grob JJ, Aaronson N, Fierbeck G, Tilgen W, Seiter S *et al*. Randomized phase III study of temozolomide versus dacarbazine in the treatment of patients with advanced metastatic malignant melanoma. *J Clin Oncol* 2000; **18**: 158–166.
- 28 Rao RD, Holtan SG, Ingle JN, Croghan GA, Kottschade LA, Creagan ET *et al*. Combination of paclitaxel and carboplatin as second-line therapy for patients with metastatic melanoma. *Cancer* 2006; **106**: 375–382.
- 29 Testori A, Rutkowski P, Marsden J, Bastholt L, Chiarion-Sileni V, Hauschild A *et al*. Surgery and radiotherapy in the treatment of cutaneous melanoma. *Ann Oncol* 2009; **20**: vi22–vi29.
- 30 Bhoumik A, Takahashi S, Breitweiser W, Shiloh Y, Jones N, Ronai Z. ATM-dependent phosphorylation of ATF2 is required for the DNA damage response. *Mol Cell* 2005; **18**: 577–587.
- 31 Eiro N, Bermudez-Fernandez S, Fernandez-Garcia B, Atienza S, Beridze N, Escaf S *et al*. Analysis of the expression of interleukins, interferon beta, and nuclear factor-kappa B in prostate cancer and their relationship with biochemical recurrence. *J Immunother* 2014; **37**: 366–373.
- 32 Snijders AM, Langley S, Mao JH, Bhatnagar S, Bjornstad KA, Rosen CJ *et al*. An interferon signature identified by RNA-sequencing of mammary tissues varies across the estrous cycle and is predictive of metastasis-free survival. *Oncotarget* 2014; **5**: 4011–4025.
- 33 Ryu H, Oh JE, Rhee KJ, Baik SK, Kim J, Kang SJ *et al*. Adipose tissue-derived mesenchymal stem cells cultured at high density express IFN-beta and suppress the growth of MCF-7 human breast cancer cells. *Cancer Lett* 2014; **352**: 220–227.
- 34 Maeda S, Wada H, Naito Y, Nagano H, Simmons S, Kagawa Y *et al*. Interferon-alpha acts on the S/G2/M phases to induce apoptosis in the G1 phase of an IFNAR2-expressing hepatocellular carcinoma cell line. *J Biol Chem* 2014; **289**: 23786–23795.
- 35 Yue C, Xu J, Tan Estioko MD, Kotredes KP, Lopez-Otalora Y, Hilliard BA *et al*. Host STAT2/type I interferon axis controls tumor growth. *Int J Cancer* 2014; **136**: 117–126.

Supplementary Information accompanies this paper on the Oncogene website (<http://www.nature.com/onc>)